Journal of Solid State Chemistry **158,** 40–48 (2001)
doi:10.1006/jssc.2000.9054, available online at http://www.idealibrary.com on IDEAL®

Support-Promoted Stabilization of the Metastable PZT Pyrochlore Phase by Epitaxial Thin Film Growth

L'H. Hamedi,[1] M. Guilloux-Viry, and A. Perrin[2]

Laboratoire de Chimie du Solide et Inorganique Moléculaire, Institut de Chimie de Rennes, UMR 6511 CNRS, Université de Rennes 1, Campus de Beaulieu, 35042 Rennes Cedex, France

and

Z. Z. Li and H. Raffy

Laboratoire de Physique des Solides, Université de Paris Sud, Bâtiment 510, 91405 Orsay Cedex, France

Received August 1, 2000; in revised form November 7, 2000; accepted December 8, 2000

Thin films of lead zirconium titanium oxide with the Zr/Ti ratio close to 52/48 have been grown by pulsed laser deposition on epitaxial (100)CeO_2 buffered R-plane sapphire substrates. Instead of the expected perovskite structure, these films are pure cubic metastable pyrochlore phase. From X-ray diffraction in $\theta-2\theta$ mode and θ-scans it appears than the films are fully {100} oriented with a mosaicity in the range $0.8^\circ-0.9^\circ$. In-plane characterizations, including RHEED photographs, electron-channeling patterns, XRD φ-scans, and near grazing incidence XRD, are indicative of high-quality epitaxial growth, cube-on-cube, on the CeO_2 sublayer. RBS analyses show that increasing the deposition temperature in the range $560-650^\circ$C does not affect the Zr/Ti ratio, while the lead content drops significantly from Pb/(Zr + Ti) = 0.7 to 0.3 (a stoichiometry close to the composition of "$Pb(Zr_{0.52}Ti_{0.48})_3O_7$"); simultaneously, the unit-cell constant decreases monotically from 10.40 to 10.15 Å. A comparison with results obtained on a variety of other substrates suggests that the driving force that imposes the growth of the pyrochlore phase at the expense of the perovskite-like one is not related to the misfit, but to the nature of the interface at the atomic scale, due to the close structural relations between fluorite and pyrochlore. This hypothesis is confirmed by the obtention of the usual perovskite variant when a (111)CeO_2 sublayer is used.

Key Words: **metastable phase; pyrochlore; thin films; epitaxy; ferroelectrics.**

INTRODUCTION

The pulsed laser deposition (PLD) technique has been proven very effective for the growth of epitaxial thin films of perovskite-based high T_c superconductors (1–3) and is now currently used for the deposition of a number of structurally related ceramic materials (3, 4).

A typical example is the PZT (lead zirconium titanium oxide) ferroelectric material, which presents valuable potential applications in various fields, including, for instance, nonvolatile memories and optical wave guides. Such films are commonly grown on single-crystal substrates that had been shown to promote efficiently the epitaxial growth of the high T_c superconductors because of their similar building block structure closely related to that of the perovskite ABO_3-type and quite similar unit-cell constants. In fact, PZT/REBa$_2$Cu$_3$O$_7$ bilayers have been grown successfully and epitaxial relations are maintained between these two materials (5, 6).

However, in the PZT thin films, a second phase is often encountered and has been assigned to a so-called "pyrochlore" material (7, 8). The parent compound $Pb_2Ti_2O_{6+x}$ has been previously reported to precipitate as a cubic form of lead titanate during the process of devitrification of lead glasses containing 10–20% TiO_2 (9). This compound was reported as a metastable phase and, indeed, it has never been obtained as a pure bulk sample by the direct ceramic route because its stoichiometry is very close to the one of the stable perovskite $PbTiO_3$ (PT). However, as stated above, it forms commonly in equilibrium with PT in thin films of the latter. A similar structure appears as an impurity in PZT thin films and is then expected to have a composition like $Pb_2(Ti, Zr)_2O_{6+x}$, although the Ti–Zr solid solution has not yet been definitively established in this compound.

[1] Present address: Université Sidi-Mohamed Ben Abdallah, Faculté des Sciences et Techniques, Fès, Maroc.

[2] To whom correspondence should be addressed. E-mail: andre.perrin@univ-rennes1.fr. Fax: +33 2 99 63 57 04.

0022-4596/01 $35.00

We report here on the growth, on CeO_2-buffered R-plane sapphire substrates, of quasi single-crystalline thin films of the cubic pyrochlore structure and on their structural characterization.

EXPERIMENTAL

1. Selection of the Substrate

The samples reported here have been obtained in the frame of a more general study of the epitaxial growth of PZT material on various single-crystal substrates, including, for instance, $SrTiO_3$ and MgO, which are well known to promote the epitaxial growth of the perovskite-type $YBa_2Cu_3O_7$ superconductor (10). As we have obtained, reproducibly, high-quality epitaxial thin films of $YBa_2Cu_3O_7$ on CeO_2/R-sapphire (i.e., $(1\bar{1}02)Al_2O_3$) (11), we were especially stimulated to study the growth of ferroelectric PZT on such substrates because the mismatch between PZT and CeO_2 is reasonable, 5.6% for the morphotropic composition $Pb(Zr_{0.52}Ti_{0.48})O_3$.

2. Growth Procedure

Thin films have been grown using PLD equipment including a stainless steel (MECA 2000) chamber with a base pressure of 10^{-6} Torr and a Xe–Cl ($\lambda = 308$ nm) excimer laser (SOPRA 502). Details on this device have been reported previously (2).

The laser beam was focused on a homemade disk, 25 mm in diameter and about 5 mm thick. A CeO_2 target was sintered in air at 1500°C for 12 h (11) and was about 90% of the theoretical density. PZT targets were designed for the growth of $PbZr_{0.52}Ti_{0.48}O_3$: the starting oxides were ground together, fired at 850°C for 2 h, reground with 5% in weight of PbO, pressed in pellets, and sintered at 1200°C for 4 h. Such a small amount of lead oxide is added to enhance densification and to reduce the lead oxide loss during the process (12). After sintering, the pellets were about 73% of the theoretical density and the lead excess had practically disappeared.

As previously reported (11), sapphire substrates were simply cleaned in acetone, glued on a stainless steel holder with silver paste, and outgassed in the deposition chamber. The CeO_2 buffer layers (typically 22 nm thick for a deposition time of 2 min) were grown at a substrate temperature of 780°C and an oxygen pressure of 0.4 mbar, with a target–substrate distance of 45 mm. These CeO_2 layers have high-crystalline quality, comparable to data previously reported in Ref. (11).

By use of a multitarget exchanger, PZT was immediately deposited *in situ* on the as-grown CeO_2 layer. The deposition time was fixed at 20 min and the oxygen pressure at 0.5 mbar. The laser fluence was set at 5 J/cm^2, the recurrence at 2 Hz, and the target–substrate distance at 45 mm, as in the case of the buffer layer deposition. After deposition, at substrate holder temperatures between 560 and 720°C, the samples were cooled at 12°C/min under increasing oxygen pressure (40 Torr/min) up to 620 Torr.

3. Characterizations

The surface smoothness of the bilayers was examined by scanning electron microscopy (SEM) at quite low voltage (6–12 KV) using a JEOL 6400 instrument and quantified by atomic force microscopy (AFM) using a Park Instrument device in contact mode. The structure of the sample was routinely studied by X-ray diffraction (XRD), including (θ–2θ (Cu$K\alpha_1$ radiation) scans and θ scans, which give information on the synthesized phases, growth direction, and mosaicity effects. In-plane ordering has been checked *in situ* by a Riber 10-KeV RHEED (reflection high-energy electron diffraction) operating around 10^{-6} Torr after cooling and *ex situ* by electron-channeling patterns (ECP). Epitaxial relationships and in-plane unit-cell constants have been determined on selected films by φ-scans diffraction and near grazing incidence diffraction using a Philips PW3373 four-circle texture diffractometer.

Selected samples have been submitted to RBS (Rutherford backscattering spectrometry) analysis carried out on Aramis accelerator (Orsay) (13) to determine their stoichiometry and thickness.

RESULTS

As-grown thin films of the lead titanium zirconium oxide are glossy, light yellow, and fully transparent. They are quite hard and well adherent: they are not stripped by the adhesive tape test. The composition of the films, deduced from RBS data, is strongly sensitive to the deposition temperature, as shown in Fig. 1. In any case, a significant amount of lead is lost, increasing with substrate temperature, and

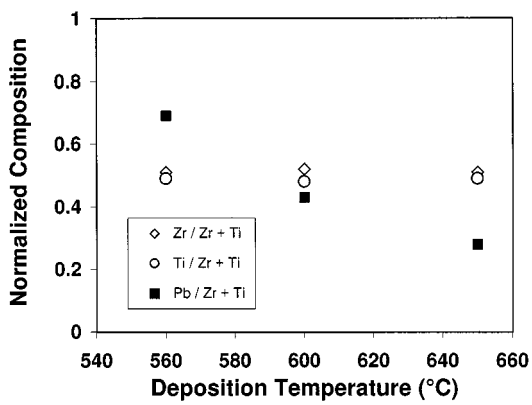

FIG. 1. Thin film composition, normalized to the Zr + Ti content (atomic), as a function of deposition temperature.

above 700°C, the films contain no more Pb: from XRD data, they appear formed by the orthorhombic ($a = 4.804$, $b = 5.482$, $c = 5.031$ Å (14)) $Ti_{\sim 0.5}Zr_{\sim 0.5}O_2$ mixed oxide strongly textured along the [100], [001], and possibly the [010] directions (the latter is difficult to prove due to the severe overlap with CeO_2 diffraction). Correlatively, the thickness of the films, evaluated from RBS data, drops from 48 to 32 nm when a significant amount of Pb has been lost.

SEM micrographs displayed in Fig. 2 show that the films are quite smooth and their topography changes slightly with deposition temperature. One can notice, for the film grown at 600°C, the presence of some small, well-defined octahedral-shaped single crystals. Meanwhile, these crystals closely resemble octahedra assigned to a pyrochlore material by Gupta and Viehland (15) and also to PbO_2 particles observed on the surface of electrochemically oxidized $Pb_2Ru_2O_7$ (16). Unfortunately, these crystals are too small to be analyzed by EDS (energy-dispersive spectrometry). However, the latter hypothesis seems unlikely because our films have a clear tendency to be lead-deficient (refer to Fig. 1). At intermediate temperatures, the films are smooth and featureless but, above 700°C, they exhibit elongated grains, clearly aligned along two perpendicular directions.

More quantitative data on the roughness have been derived from AFM micrographs displayed in Fig. 3. General similar behavior is observed, and data reported in Fig. 4 show that the roughness of the films, typically around 1–2 nm rms, sharply increases to 5 nm for films deposited above 700°C, i.e., when the lead content starts to vanish.

Figure 5 reproduces the typical θ–2θ scan of a representative sample. Besides the expected $(1\bar{1}02)$ and $(2\bar{2}04)$ sapphire and (200)CeO_2 peaks, only one reflection is observed at 34.48° for the film deposited at 560°C. This value is very close to the diffraction angle usually assigned to the (400) reflection of the pyrochlore structure and corresponds to an unit-cell constant of 10.40 Å: this value is very close to the

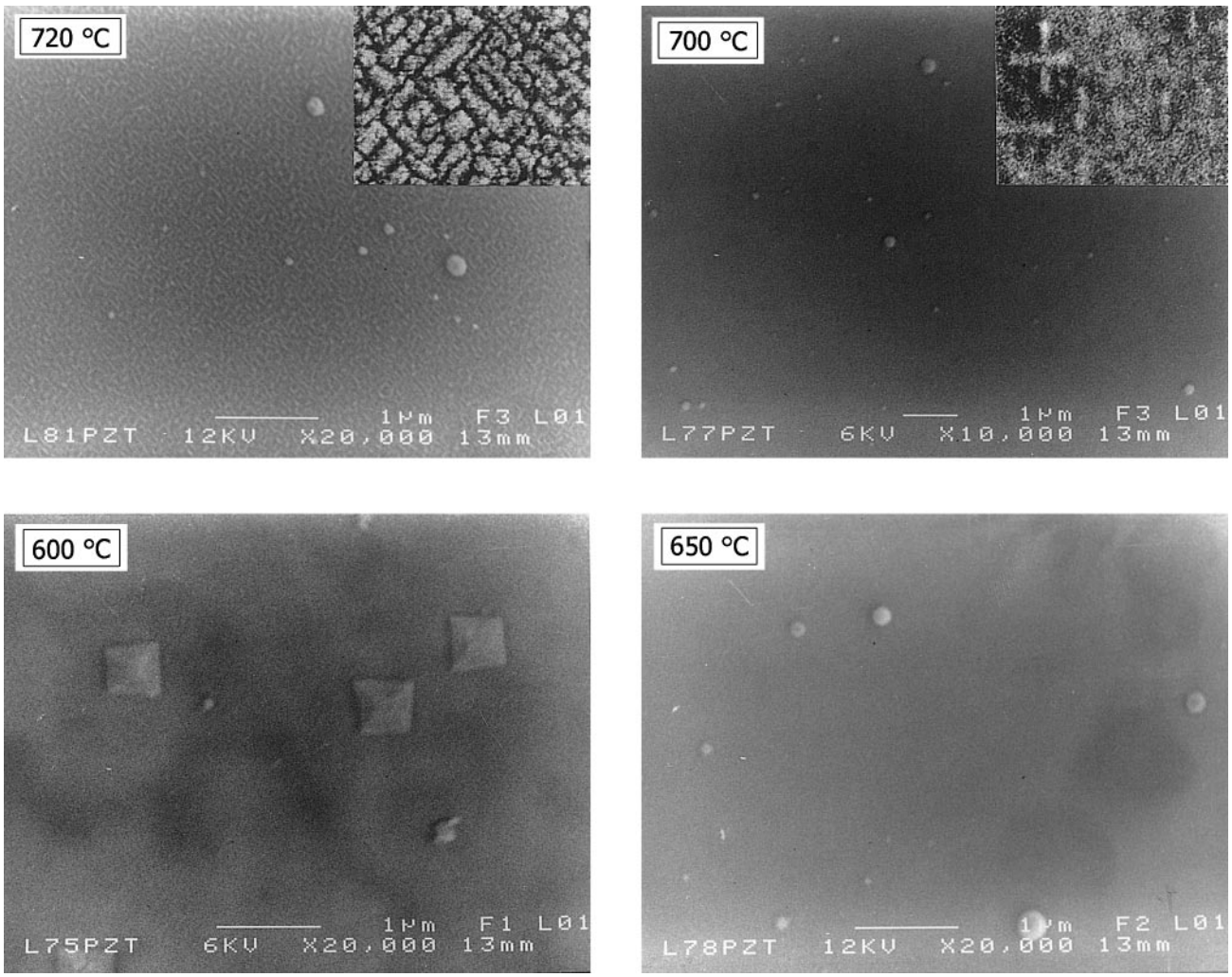

FIG. 2. SEM micrographs of thin films grown at various temperatures at $G \times 20{,}000$ (insets are photographs obtained at $G \times 100{,}000$ using a FEG instrument). Scattered submicrometer droplets are characteristic of the pulsed laser deposition process.

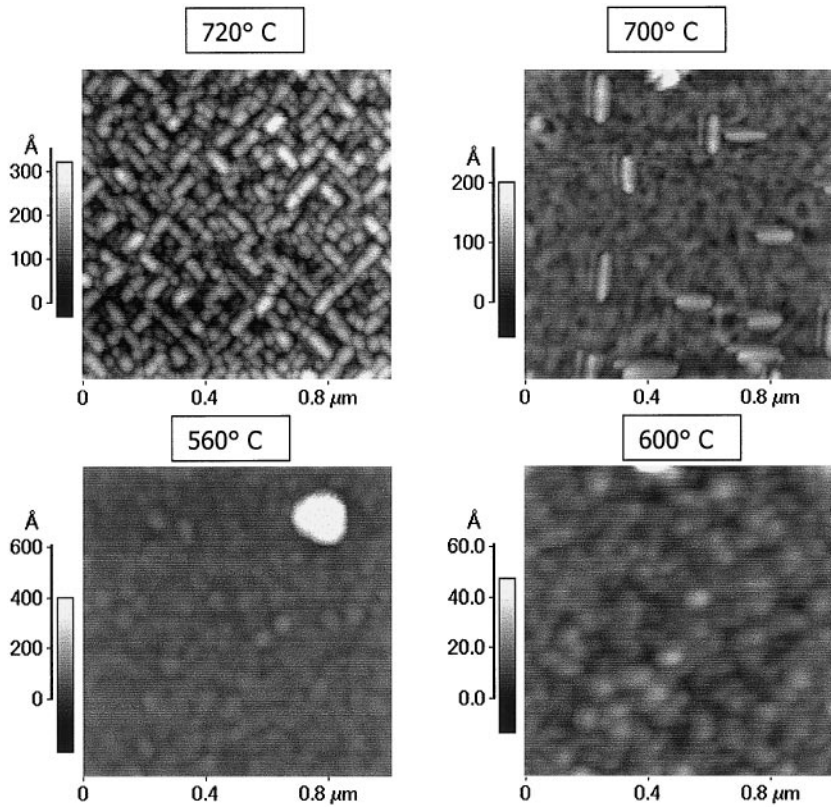

FIG. 3. AFM micrographs of films grown at various temperatures. Compare to insets to Fig. 2.

reported unit-cell constant of $Pb_2Ti_2O_6$ (9). The arrows in Fig. 5 mark the expected diffraction angles for the 001 and 002 reflections of the PZT perovskite structure: the latter is obviously absent in this sample and has never been observed on this CeO_2/Al_2O_3 substrate, whatever are our growth conditions. It is then concluded that these films consist in the strongly oriented pyrochlore phase, grown along the $\langle 100 \rangle$ direction.

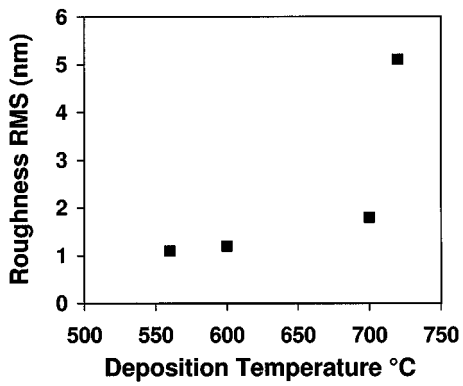

FIG. 4. Evolution of rms roughness of the films as a function of deposition temperature.

Rocking curves (θ-scans) are quite narrow (see inset to Fig. 6), typically around 0.8° FWHM (full width at half-maximum), to be compared to an average value of 0.02° for the substrate and 0.04° for the CeO_2 layer: this indicates reasonable mosaic effects along the growth direction. The θ-scan peaks tend to narrow when the deposition temperature increases, as shown in Fig. 6.

Wide-angle ECP patterns, although strongly distorted due to considerable charging-up effects, the signature of dielectric materials, exhibit a sharp contrast, the presence of high-order index stripes, and a fourfold symmetry (Fig. 7): these results prove a well-defined in-plane ordering, i.e., an epitaxial-like growth. Indeed, the RHEED patterns recorded for films grown between 560 and 700°C present usually narrow streaks indicative of smooth surfaces and in-plane ordering (Fig. 8). From the streaks separation an in-plane unit-cell constant close again to 10.3 Å is deduced, suggesting the possibility of a cubic lattice. To check the validity of this assumption, a detailed study of the structure of the film, using tilted XRD configuration, has been carried out.

Figure 9a is the φ-scan of the 404 reflection of the pyrochlore phase, obtained at a tilt angle $\psi = 45°$, a value which suggests again a cubic unit cell. The associated 2θ value of 50.20° is in good agreement with the 10.28 Å unit-cell

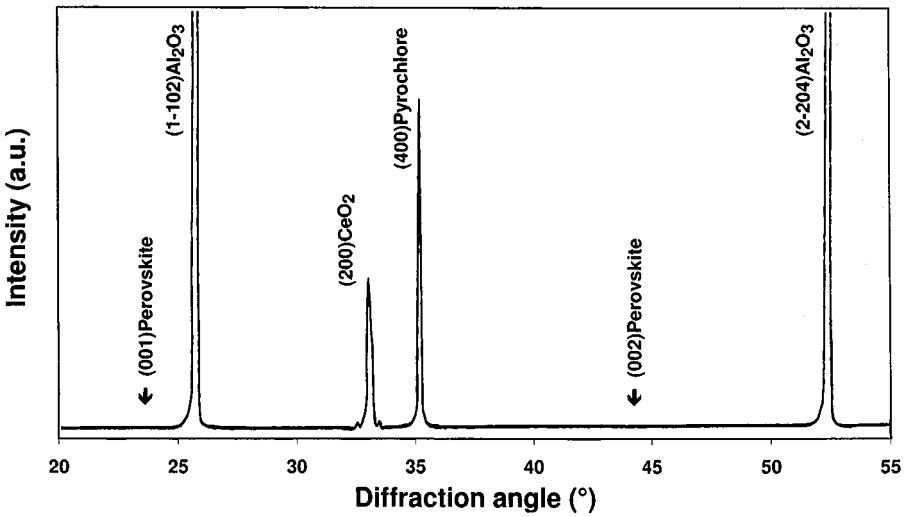

FIG. 5. Typical XRD θ–2θ scan (Cu$K\alpha_1$ radiation) of a pyrochlore film deposited at 560°C. The arrows mark the expected positions of the 001 reflections of the standard PZT perovskite phase.

constant determined from symmetric θ–2θ scan for this sample, grown at 600°C. Four sharp peaks are observed each 90°, a proof of the epitaxial growth of the pyrochlore layer. As shown by comparison with Fig. 9b, relative to the φ-scan of the CeO_2 underlayer ($\{202\}$ reflection at $\psi = 45°$ and $2\theta = 47.48°$), the diffraction azimuths are the same, meaning a cube-on-cube growth of the two materials.

Finally, near grazing incidence experiments have been carried out to measure directly the in-plane unit-cell constants. Figure 10 shows the φ-scan obtained at a tilt angle $\psi = 88.4°$: the four peaks, corresponding to 040 and 004, are spaced 90° and also agree with two identical values of the in-plane unit-cell constants, as expected for a cubic structure. Figure 11 is the θ–2θ scan recorded for one of those peaks, confirming the 2θ value of 34.89° and then $a = 10.27$ Å. Furthermore, a θ–2θ scan obtained at $\varphi = 45°$ apart from the former peaks exhibited, for $2\theta = 50.20°$, the $\{440\}$ planes diffraction, as expected (see inset to Fig. 11).

Comparison of the standard θ–2θ scans for films grown at increasing temperatures reveals that the 400 peak shifts to a larger diffraction angle. Figure 12 shows that the out-of-plane a unit-cell constant monotically decreases from about 10.40 to about 10.16 Å when the deposition temperature increases from 560 to 700°C. In the same range of temperature, the mosaicity of the films tends to slightly improve, as mentioned above (report to Fig. 6).

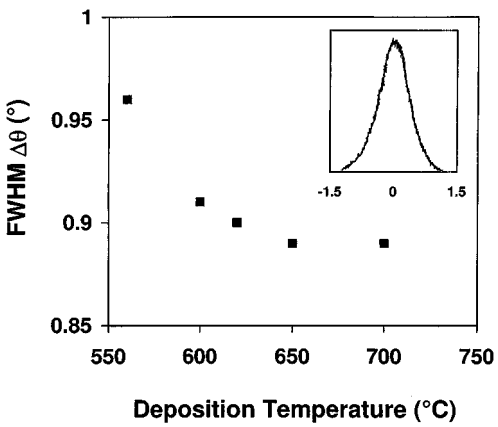

FIG. 6. Full width at half-maximum of the rocking curves (inset) of pyrochlore films deposited at various temperatures.

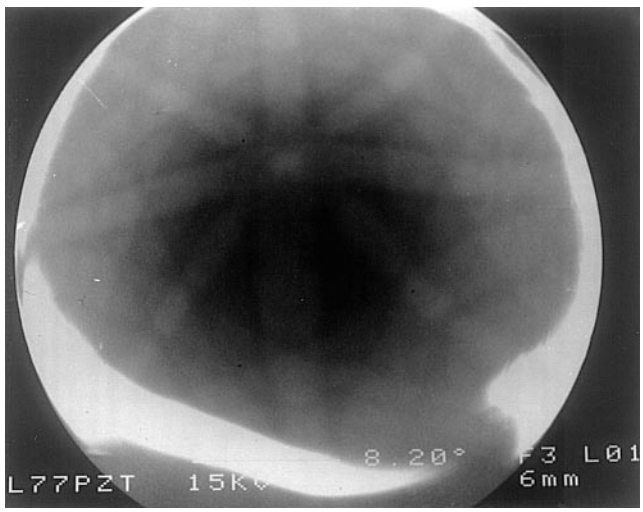

FIG. 7. Typical wide-angle channeling pattern, relative to a film grown at 700°C. The distortion of the pattern is due only to severe charging-up effects: it is suppressed by the deposition of a thin conductive overlayer, but at the expense of sharpness loss, especially concerning high-order index stripes.

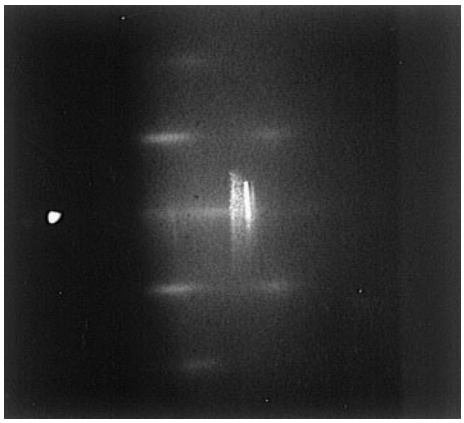

FIG. 8. Typical RHEED pattern of the pyrochlore films grown in the 560–700°C range of deposition temperature.

DISCUSSION

In this work we have obtained in the form of thin films quasi-single-crystal samples of the so-called metastable pyrochlore phase in the lead zirconium titanium oxide system.

Much is to be known about this phase, often encountered in the PT as well as the PZT system, especially in the field of thin films growth. Indeed, as stated above, a phase of this type has been obtained in the process or devitrification of silica glasses having high lead and titanium contents (9). In this early work, the obtained powdered sample was assumed to present the pyrochlore structure on the basis of the indexation of the XRD patterns and to have the composition $Pb_2Ti_2O_6$ (meaning an oxygen-deficient pyrochlore), which is exactly the same stoichiometry as the PT perovskite-based compound. However, the possible presence of extra Ti was not ruled out. This phase was reported to be metastable and to transform, without oxygen evolution, to the perovskite structure at about 620°C. Indeed, the pyrochlore structure is not obtained via the ceramic route and is absent from the phase diagrams established at 1100–1200°C and reported for instance by Kingon and Clark (17). In contrast, when firing a mixture of

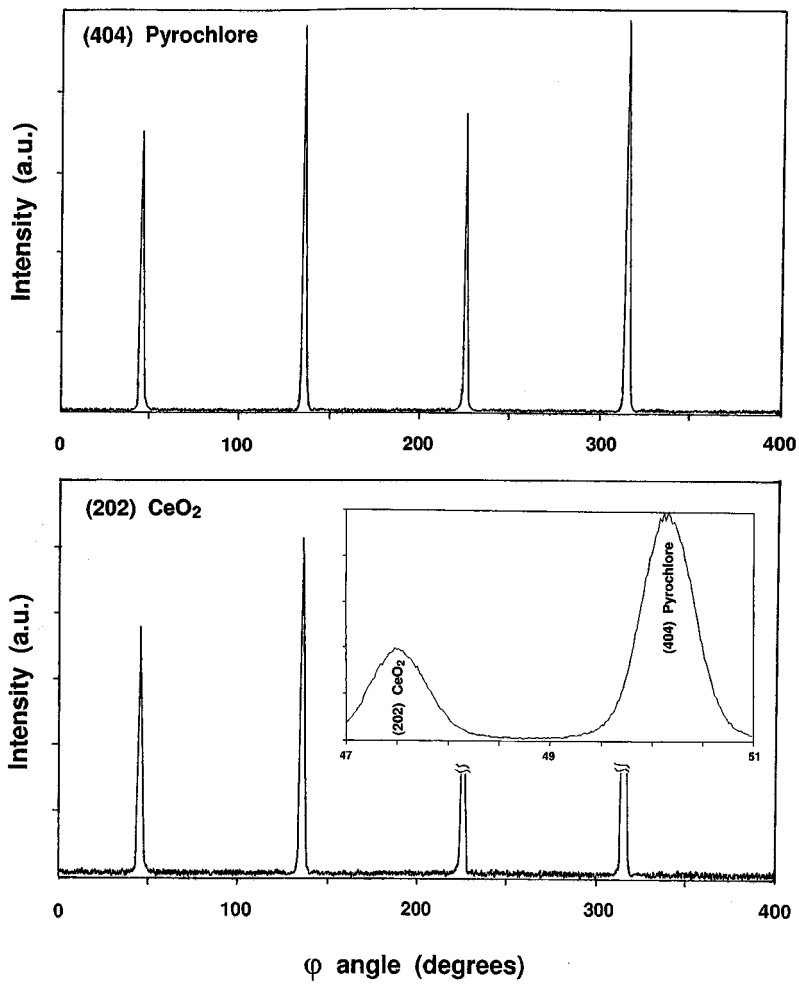

FIG. 9. XRD pattern in the φ-scan mode (at $\psi = 45°$) of the 404 reflection of the pyrochlore phase at $2\theta = 50.20°$ (top), compared to the φ-scan of the 202 reflection of the CeO_2 underlayer at $2\theta = 47.48°$ (bottom). The inset shows the θ–2θ scan taken at an azimuth $\varphi(I_{max})$ for the same angle of tilt ψ.

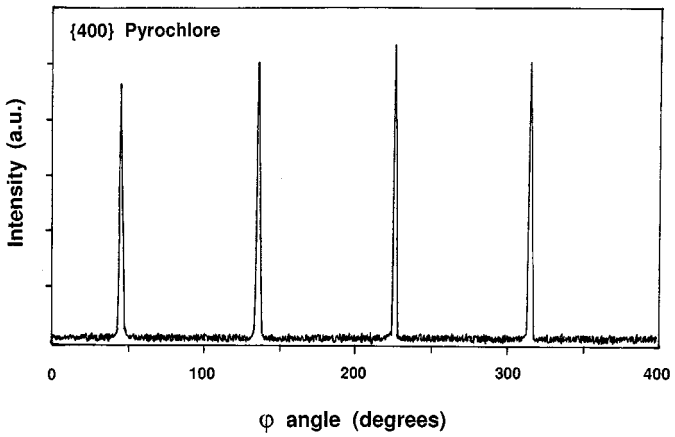

FIG. 10. XRD pattern in the φ-scan mode at a near grazing incidence ($\psi = 88.4°$) of a pyrochlore film: the four peaks correspond to {400} reflections and are spaced 90°.

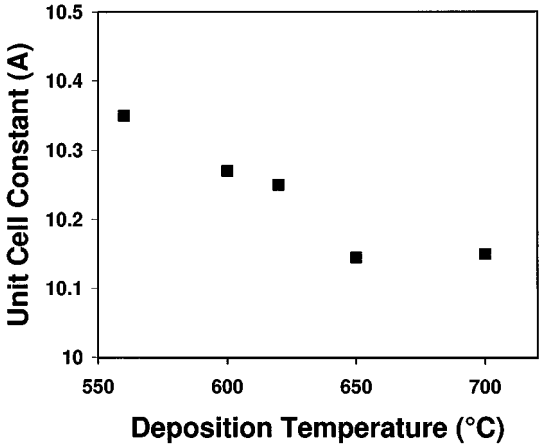

FIG. 12. The variation of the out-of-plane a unit-cell constant of pyrochlore films with the deposition temperature.

metalorganic precursors of lead, zirconium, and titanium (Zr/Ti = 0.53:0.47) at 500°C, Klee *et al.* (7) obtained either nearly pure perovskite powder or a mixture of both perovskite and pyrochlore phases, depending on the two sets of starting compounds they used. On the other hand, starting from a sol–gel precursor based on lead acetate, they obtained, at the same temperature, the pure, but poorly crystallized, pyrochlore variant, with a unit-cell constant of 10.51 Å. All these powders irreversibly transformed to the perovskite structure when heated above 600°C.

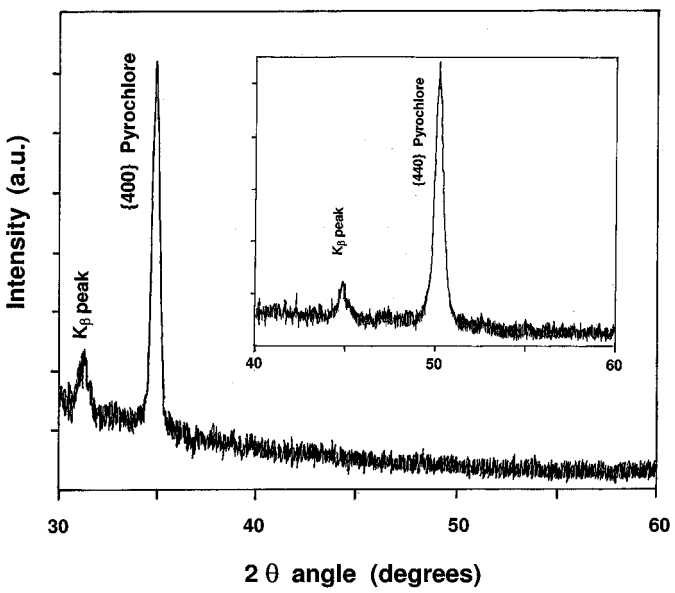

FIG. 11. XRD pattern recorded in the θ–2θ mode for the $\varphi(I_{max})$ and ψ setting angles corresponding to Fig. 10 and relative to a {400} reflection of the pyrochlore. The inset is the XRD pattern taken at $\varphi + 45°$ and is relative to a {440} reflection. The K_β peaks are observed because in this experiment the monochromator has been removed for having enough beam intensity.

In the case of thin films, the pyrochlore structure is often encountered as an undesired second phase. Its formation is understandable, taking into account the fact that PT or PZT thin films are grown at a temperature as low as possible to avoid lead losses. In addition, lead deficiency could favor the pyrochlore, as stated by Klee *et al.* (7), who obtained the pure perovskite only when they used metalorganic solutions with a Pb excess of 8–12 mol%. However, even with lead deficiency, the perovskite phase can be obtained on selected substrates, for instance, on $SrTiO_3$ (5) or LiF (18).

The actual situation could be in fact more complex. As an illustration, on (100) MgO, Lee *et al.* (19), observed successively at increasing substrate temperature the (100) + (111) oriented pyrochlore, then the perovskite, and finally again an oriented pyrochlore, with a smaller unit-cell constant, which appears above 600°C when the Pb content had significantly dropped. Similarly, in the PT system, Tabata *et al.* (20) reported the formation of the pyrochlore below 350°C, the perovskite in the range 380–550°C, and a mixture of $PbTi_3O_7$ and TiO_2 above 550°C. Also, in the case of films grown by metalorganic *ex situ* route, Chen and Chen (21) reported a pyrochlore–perovskite transformation near 550°C and a "Pb-deficient pyrochlore-type phase of $PbTi_3O_7$" appearing at a temperature as high as 800°C when PbO rapidly evaporates. It is noteworthy that the compositions we obtain in our higher temperature range of deposition tend to the formulation PbM_3O_7 (M being around 0.5 Zr + 0.5 Ti as in the target), and the films remain apparently cubic, in contrast to the expected symmetry of the latter, because bulk stoichiometric $PbTi_3O_7$ is monoclinic (22). In addition, we show that the associated cubic a unit-cell constant decreases monotically with the lead stoichiometry. This is indicative that the pyrochlore structure could present a range of composition, well explained in

TABLE 1
Misfit Values[a] of PZT (Perovskite and Pyrochlore Variants) against Various Substrates

Film structure	Substrate	Substrate structure	Misfit (%)
Perovskite	LiF	Rock salt	+0.4
	MgO	Rock salt	−4.1
	R–Al_2O_3	Corindon	−16
	R–$LaAlO_3$	Corindon	+6.5
	$SrTiO_3$	Perovskite	+3.5
	$YBa_2Cu_3O_7$	Perovskite-like	+4.8
	CeO_2	Fluorite	+5.6[b]
Pyrochlore	CeO_2	Fluorite	−3.9 to −6.2[c]

[a] According to the standard formula $f(\%) = 100\ (a_F - a_S)/a_S$.
[b] Relative to the 45° rotated substrate unit cell.
[c] Relative to substrate doubled unit cell and depending on film composition.

the hypothesis of an M substitution for Pb on the A sites of the structure, and would remain even for compositions close to PbM_3O_7 and then reformulated as $Pb_{1-x}M_xM_2O_7$ to match the standard pyrochlore structure description. It is noteworthy that, in contrast to the results reported above, the pyrochlore structure is obtained here alone in the full range of temperature, without any intermediate formation of the perovskite phase. This behavior is a strong indication that the high-temperature Pb-deficient phase would actually be a pyrochlore structure, as suggested above.

Thus, the question that arises is why the CeO_2 buffer layer so strongly promotes the growth of the pyrochlore phase as, at least in our experimental conditions, we never detect any amount of the perovskite allotrope. Table 1 summarizes the values of the unit-cell misfit between PZT perovskite type and a variety of substrates (or buffer layers) and compares them with the misfits between CeO_2 and both the perovskite and pyrochlore variants. We have grown the perovskite phase onto all these substrates, with the exception of CeO_2, which in contrast promotes very efficiently the epitaxial growth of c-axis-oriented, perovskite-like, $YBa_2Cu_3O_7$ (5). The misfit values do not appear different enough to be the prominent factor in explaining the observed results and, indeed, an independent study of the growth of the PZT system on various substrates also showed the lack of correlation between the misfit value and the relative amount of the two phases (23).

More likely, research on the selectivity of the pyrochlore structure growth on the CeO_2 fluorite structure (as well as on YSZ (23)) should include details of the interface of the two materials. Indeed, it is well known that the pyrochlore structure directly derives from the fluorite one, when the unit-cell constant is doubled and ordered vacancies are introduced both in the cationic and in the anionic subcells. The terminal plane of (100)CeO_2 is expected to be the dense plane of pure oxygen, as displayed in Fig. 13, because

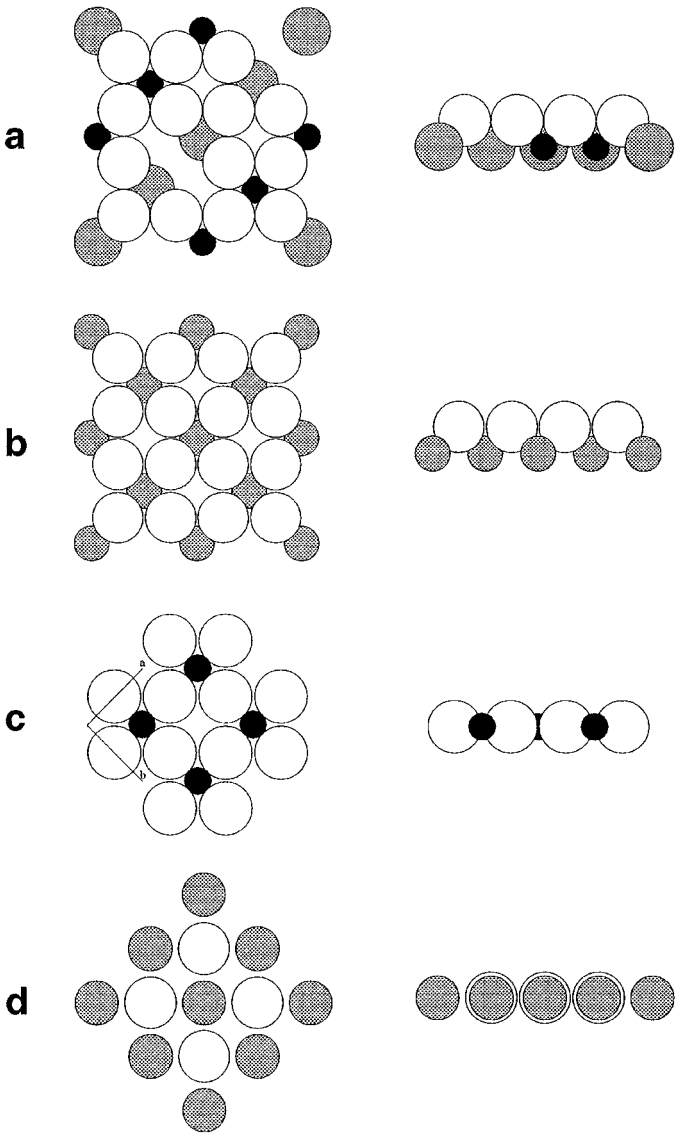

FIG. 13. A schematic representation of the expected termination planes of the pyrochlore (a) and fluorite (b) structures and of the two possible termination planes of the perovskite (c and d). On the right side are the cross sections of the corresponding interfacial planes.

a terminal plane of Ce ions would imply pendant bonds. So it is clear that the growth of the pyrochlore structure can occur on this plane without any structural discontinuity. In contrast, the two AO and BO_2 possible terminal planes of the ABO_3 perovskite structure contain both oxygen and cations, and consequently the electrostatic potential distribution near the surface is significantly different. This feature does not hinder the growth of a perovskite block on the cerine surface when only this structure can form, as in the example of $YBa_2Cu_3O_7$ superconductor, which sets 45° rotated with respect to the CeO_2 unit cell (11). In contrast, in

the PT and PZT systems where the perovskite and pyrochlore structures can compete, the latter will be strongly favored.

Further argument is the result of the growth of PZT films on the (111)CeO_2 sublayer. The latter forms preferentially on R-plane sapphire as a textured film when deposited under about 10^{-5}–10^{-6} Torr instead of some 10^{-1} Torr of oxygen (11, 24). Deposition of PZT on this (111)CeO_2 underlayer results in (101)-oriented perovskite thin films, as evidenced by XRD. These films are of course only textured, like the underlayer material: they exhibit uncontrasted ECP patterns and streaks insensitive to the electron beam azimuth in their RHEED patterns. Again, this structure and orientation can be inferred from the expected termination plane of the underlayer: indeed, the (111) plane of CeO_2 contains oxygen and cerium cations, very slightly shifted above and under the average plane position and, while distorted, resembles likely the basal planes of the perovskite structure.

ACKNOWLEDGMENTS

This work was supported in part by Fondation Langlois. SEM and EDS experiments were carried out at CMEBA, electron microscopy and microanalysis center of University of Rennes. Dr. D. Lemoine (INSA Rennes) and F. Lalu and Professor J. Lesueur (IN2P3 Orsay) are warmly acknowledged for AFM and RBS experiments, respectively.

REFERENCES

1. D. Dijkkamp, T. Venkatesan, X. D. Wu, N. Shaheen, N. Jisrawi, Y. H. Min-Lee, W. L. McLean, and M. Croft, *Appl. Phys. Lett*. **51,** 619 (1987).
2. M. G. Karkut, M. Guilloux-Viry, A. Perrin, J. Padiou, and M. Sergent, *Physica C* **179,** 262 (1991).
3. O. Auciello, "Handbook of Crystal Growth" (D. J. T. Hurle, Ed.), Vol. 3, Chap. 9, p. 365. North Holland, Amsterdam, 1994.
4. M. Guilloux-Viry and A. Perrin, "Recent Research Developments in Crystal Growth Research" (S. G. Pandalai, Ed.), Vol. 2, Chap. 1, p. 1. Transworld Research Network, Trivandrum, 2000.
5. L'H. Hamedi, M. Guilloux-Viry, A. Perrin, and M. H. Cherkani, *Ann. Chim. Sci. Mater*. **23,** 377 (1998).
6. J.-M. Triscone, L. Frauchiger, M. Decroux, L. Miéville, Ø. Fischer, C. Beeli, P. Stadelmann, and G.-A. Racine, *J. Appl. Phys.* **79,** 4298 (1996).
7. M. Klee, R. Eusemann, R. Waser, W. Brand, and H. van Hal, *J. Appl.* Phys. **72,** 1566 (1992).
8. S. B. Krupanidhi, H. Hu, and V. Kumar, *J. Appl. Phys.* **71,** 376 (1992).
9. F. W. Martin, *Phys. Chem. Glasses* **6,** 143 (1965).
10. A. Perrin, M. Guilloux-Viry, C. Thivet, and M. Sergent, *in* "Studies of High T_c Superconductors," (A. V. Narlikar, Ed.), Vol. 13, Chap. 1, pp. 1–62, Nova Science, 1994.
11. X. Castel, M. Guilloux-Viry, A. Perrin, J. Lesueur, and F. Lalu, *J. Cryst. Growth* **187,** 211 (1998).
12. B.-M. Song, D.-Y. Kim, S.-I. Shirasaki, and H. Yamamura, *J. Am. Ceram. Soc*. **72,** 833 (1989).
13. E. Cottereau, J. Chaumont, R. Meunier, and H. Bernas, *Nucl. Inst. Methods B* **45,** 223 (1990).
14. P. Bordet, A. Mc Hale, A. Santoro, and R. S. Roth, *J. Solid State Chem.* **64,** 30 (1986).
15. S. M. Gupta and D. Viehland, *J. Am. Ceram. Soc*. **80,** 477 (1997).
16. G. Gokagac and B. J. Kennedy, *J. Electroanal. Chem.* **368,** 235 (1994).
17. A. I. Kingon and J. B. Clark, *J. Am. Ceram. Soc*. **66,** 253 (1983).
18. L'H. Hamedi, M. Guilloux-Viry, A. Perrin, and G. Garry, *Thin Solid Films* **352,** 66 (1999).
19. J. Lee, A. Safari, and R. L. Pfeffer, *Appl. Phys. Lett*. **61,** 1643 (1992).
20. H. Tabata, T. Kawai, S. Kawai, O. Murata, J. Fujioka, and S. Minakata, *Appl. Phys. Lett*. **59,** 2354 (1991).
21. S. Y. Chen and I. W. Chen, *J. Am. Ceram. Soc*. **77,** 2337 (1994).
22. K. Kato, I. Kawada, and K. Muramatsu, *Acta Crystallogr. B* **30,** 1634 (1974).
23. W. Biegel, R. Klarmann, M. Hanika, K. Sturm, and B. Stritzker, *Mater. Sci. Eng. B* **56,** 195 (1998).
24. A. G. Zaitsev, G. Ockenfuss, D. Guggi, and R. Wördenweber, *J. Appl. Phys.* **81,** 3069 (1997).